

Functionalized Fe₃O₄ Nanoparticles for Detecting Zinc Ions in Living Cells and Their Cytotoxicity

Gyusik Kang,^[a] Hyunjong Son,^[a] Jung Mi Lim,^[b] Hee-Seek Kweon,^[c] In Su Lee,^[d] Dongmin Kang,^{*[b]} and Jong Hwa Jung^{*[a]}

The design and synthesis of metal chemosensors with high selectivity and sensitivity is an active field in supramolecular chemistry.^[1] Particular attention has been focused on heavy and/or transition metal (HTM) ions and their detection in the cell environment.^[2] Zinc(II) ions are the second most abundant transition metal ions essential for the human body and play an indispensable role in various biological processes, such as gene transcription, regulation of metalloenzymes, cell apoptosis, neural signal transmission, and insulin secretion.^[3] The total concentration of Zn²⁺ varies widely in different types of cells, ranging from the nanomolar level to approximately 0.3 mM.^[4] The detection and imaging of Zn²⁺ in biological samples are of significant interest due to this cation's unique role in physiological functions. Numerous scientific endeavors have focused on the development of fluorescent chemosensors for the *in vitro* and *in vivo* detection of Zn²⁺.^[5] For example, Yoon et al. have recently reported a highly selective, cell permeable, and ratiometric fluorescent probe for Zn²⁺.^[6] However, some of the reported Zn²⁺ probes have poor water solubility and are vulnerable to interference by the presence of other metal ions. Furthermore, the majority of existing probes might not be able to perform within the cell environment. Therefore, the development of fluorescent probes with greater versatility and improved performance is still in great demand.

Magnetic nanoparticles are of great interest for biomedical and environmental research applications, such as bioseparation, drug targeting, cell isolation, enzyme immobiliza-

tion, and protein purification, because of their biocompatibility and stability against degradation.^[7] Receptor-immobilized magnetic nanoparticles have some important advantages as solid chemosensors and adsorbents in heterogeneous solid–liquid phases.^[8] First, such nanoparticles are readily synthesized by hydrolysis reactions—a versatile technique that allows introduction of chemical functionalities. Second, immobilized receptors on inorganic nanoparticles can remove guest molecules (toxic metal ions and anions) from the pollutant solution. Third, magnetic nanoparticles can be easily isolated and controlled from pollutants by a small magnet and can be repeatedly utilized with suitable regenerative treatment. Magnetic nanoparticles can also provide efficient binding to guest molecules because of their high surface-to-volume ratio, which simply offers more contact area.

With these concepts in mind, we undertook the construction of a new magnetic nanoparticle-based OFF–ON fluorescent Zn²⁺ probe (**1**) that operates by a photoinduced electron transfer (PET) mechanism. Probe **1** was shown to be highly selective for Zn²⁺ in aqueous media. The application of this new magnetic nanoparticle-based probe for the detection of zinc ions in living cells is also described. To obtain a highly selective OFF–ON probe for Zn²⁺ in aqueous solution for practical applications, we introduced a BODIPY moiety as the fluorophore because of its characteristically strong fluorescence behavior (including high fluorescence quantum yields) and its high chemical stability. Fe₃O₄ nanoparticles were employed as the inorganic support because of their noncytotoxicity and the ease of their magnetic separation.

The overall synthesis procedure for nanomaterials **1** is depicted in Scheme 1. First, we prepared the supporting nanomaterials from superparamagnetic Fe₃O₄ nanoparticles of about 20 nm in diameter stabilized by oleic acid through

[a] G. Kang, H. Son, Prof. Dr. J. H. Jung

Department of Chemistry and Research Institute of Natural Sciences Gyeongsang National University
Jinju 660-701 (Korea)
E-mail: jonghwa@gnu.ac.kr

[b] J. M. Lim, Prof. Dr. D. Kang

Division of Life and Pharmaceutical Sciences
Ewha Women's University, Seoul 120-750 (Korea)
E-mail: dkang@ewha.ac.kr

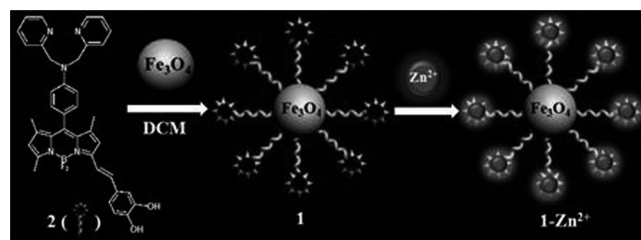
[c] Dr. H.-S. Kweon

Division of Electron Microscopic Research
Korea Basic Science Institute, Daejeon 305-333 (Korea)

[d] Prof. Dr. I. S. Lee

Department of Chemistry
Pohang University of Science and Technology
Nam-Gu, Pohang 790-784 (Korea)

Supporting information for this article is available on the WWW under <http://dx.doi.org/10.1002/chem.201200294>.



Scheme 1. Preparation of BODIPY-functionalized Fe₃O₄ nanoparticles (**1**).

a previously reported procedure.^[8b,c,d] The BODIPY-based derivative was selected as the fluorogenic group due to its sharp fluorescence peaks with high quantum yields, and insensitivity to the polarity and pH of the environment. Secondary, compound **3** was synthesized by following a similar method to that described previously (Scheme S1 in the Supporting Information).^[9] Then, compound **3** was treated with 3,4-dihydroxy benzaldehyde in the presence of acetic acid and piperidine to give the desired product **2** in toluene. Third, the Fe₃O₄ nanoparticles were treated with **2** in toluene with vigorous stirring, overnight, to link them onto the surface of the Fe₃O₄ nanoparticles by covalent bonding (see the Experimental Section and Scheme 1). Finally, **1** was fully characterized by transmission electron microscopy (TEM), FTIR spectroscopy, time-of-flight second ion mass spectroscopy (ToF-SIMS), and fluorophotometry.

TEM imaging of **1** revealed a spherical structure with a narrow size distribution (ca. 20 nm) that maintained its nanocrystalline appearance (Figure 1). The IR and ToF-

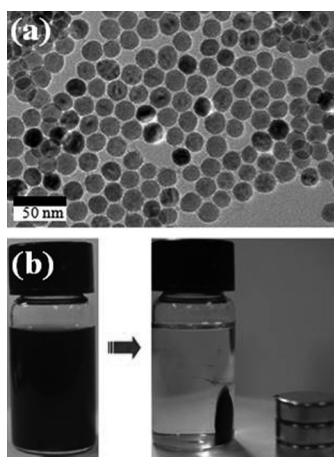


Figure 1. a) TEM image of **2**-immobilized Fe₃O₄ nanoparticles (**1**); scale bar: 50 nm. b) Photograph of a magnet attracting **1** in aqueous solution.

SIMS results were in accord with bond formation; the IR spectrum of **1** showed strong new bands at 3469, 3313, 3145, 3003, 2927, 2833, 2591, 2553, 2455, 1484, 1465, 1235, 1162, and 1043 cm⁻¹, which originated from receptor **2**; this is in accord with **2** residing on the Fe₃O₄ nanoparticles (Figure S1 in the Supporting Information). The ToF-SIMS spectrum of **1** displayed fragments attributable to **2** (*m/z* 414 and 441), and thereby provides evidence that **2** was anchored onto the surface of the Fe₃O₄ nanoparticles (Figure S2 in the Supporting Information).

Spectroscopic measurements for **1** were performed in HEPES (4-(2-hydroxyethyl)-1-piperazineethanesulfonic acid; 20 mM) buffer, pH 7.4. The UV/Vis absorption spectrum of free **1** showed one absorption band at 570 nm ($\epsilon = 4.17 \times 10^4 \text{ M}^{-1} \text{ cm}^{-1}$). As expected, nanoparticle **1** is virtually nonfluorescent in its apo state ($\Phi < 0.0018$, $\lambda_{\text{ex}} = 570 \text{ nm}$), which is a consequence of the efficient PET^[10] quenching of the fluorophore by the lone-pair electrons of the nitrogen

atom in the benzoyl moiety. Upon addition of increasing Zn²⁺ concentrations, **1** showed a large chelation-enhanced fluorescence (CHEF) effect in the fluorescence emission spectra; this results from the blocking of the PET process and we observed an overall emission increase of approximately 32-fold ($\Phi = 0.058$, Figure 2) at the emission maximum ($\lambda_{\text{em}} = 594$).

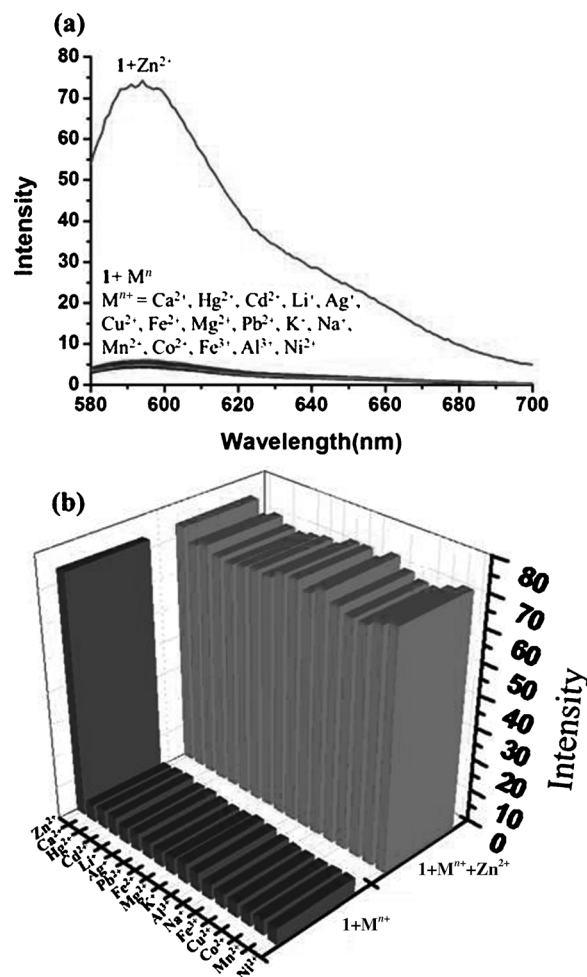


Figure 2. a) Fluorescence changes of **1** (10 μM) upon addition of Zn²⁺ ions in the presence of other metal ions (150 equiv) in aqueous solution. b) Fluorescence responses of **1** to various metal ions. The bars labeled as **1**+Mⁿ⁺ represent the addition of selected metal ions (150 equiv) to a solution of **1** (10 μM). The bars labeled as **1**+Mⁿ⁺+Zn²⁺ represent subsequent addition of Zn²⁺ (150 equiv) to the solution. For all measurements, the pH value was adjusted by using HEPES (20 mM) in pure aqueous solution, pH 7.4. Excitation was achieved at 570 nm, and the emission was monitored at 594 nm.

With few exceptions,^[11] most reported BODIPY-fluorescent probes are based on an intramolecular charge transfer (ICT) mechanism.^[10] However, in our case, the noticeable fluorescence intensity enhancement of receptor **2** attached to Fe₃O₄ nanoparticles can be due to the inhibition of the PET process, which quenches fluorescence, during the binding of Zn²⁺. Preliminary computational simulations indicated that **2** is twisted at the BODIPY moiety; this presumably

results in a blocking of the ICT. In addition, the direct conjugation of the amine to the styryl group results in a very significant red shift, and high fluorescence quantum yields for this BODIPY-based receptor.^[10a]

We also investigated the ability of **1** to serve as an ion-selective fluorogenic probe by testing the binding of other metal ions, including Ca^{2+} , Hg^{2+} , Cd^{2+} , Li^+ , Ag^+ , Cu^{2+} , Fe^{2+} , Mg^{2+} , Pb^{2+} , K^+ , Na^+ , Mn^{2+} , Co^{2+} , Fe^{3+} , Al^{3+} , and Ni^{2+} . However, no significant spectral changes were observed upon addition of any of these metal ions (Figure 2); this indicates that nanoparticle **1** is a highly selective chemoprobe for the detection of Zn^{2+} .

For comparison, we performed spectroscopic measurements using ligand **2** in acetonitrile solution (**2** was insoluble in water); under these conditions **2** gave a single absorption band at 570 nm ($\epsilon = 5.0 \times 10^4 \text{ M}^{-1} \text{ cm}^{-1}$). In the absence of Zn^{2+} , **2** also exhibited no fluorescence emission when excited at 570 nm. Upon the addition of Zn^{2+} , the fluorescence emission intensity of **2** increased by approximately 1.5-fold ($\Phi = 0.0045$, Figure S3 in the Supporting Information) with an emission maximum at 594 nm. Other metal ions, such as Ni^{2+} , Hg^{2+} , and Al^{3+} , also induced the fluorescence intensity enhancement of **2**. In particular, the fluorescence enhancement of **1** upon the addition of Al^{3+} can occur because the two hydroxyl groups of BODIPY dye act as binding sites for Al^{3+} . Al^{3+} can be classified as a hard acid by HSAB theory.^[12] The lower selectivity of **2** for Zn^{2+} compared to **1** can be attributed to its high flexibility and its acyclic structural character prior to immobilization on the surface of the nanoparticles.

The highly selective Zn^{2+} recognition of nanoparticle-based fluorescence chemoprobe **1** demonstrates that the approach employed in the present study cooperatively enhances and controls the selectivity towards this metal ion. More importantly, quantitative measurements of the emission maximum of Zn^{2+} -bound **1** indicated that the fluorescence change correlated linearly with the $[\text{Zn}^{2+}]$ over the 0–30 ppb range investigated. As shown in Figure S4 in the Supporting Information, the detection limit for Zn^{2+} is approximately 0.2 nM. Considering that the Zn^{2+} concentration in living cells can vary from nanomolar levels to about 0.3 mM, the observed detection limit for nanoparticle **1** in aqueous media could be highly advantageous under certain circumstances. Evaluation of the time course for the fluorescence intensity of nanoparticle **1** at 594 nm (Figure S5 in the Supporting Information) indicated that immediately after the addition of Zn^{2+} , its fluorescence intensity started to increase, and that by 60 s the fluorescence intensity was almost saturated. Thus, the response time of this system is within 1 min; this makes it a rapid and convenient method for the quantification of Zn^{2+} in aqueous solutions (Figure S5 in the Supporting Information).

After exposure to Zn^{2+} , nanoparticle **1** was successfully regenerated. When the Zn^{2+} -bound nanoparticle **1** was treated with an aqueous EDTA solution (10 μM), the fluorescence intensity of Zn^{2+} -bound nanoparticle **1** was quenched. However, when the washed, stripped nanoparti-

cle **1** were re-exposed to Zn^{2+} , the fluorescence emission was again present, with no reduction in response (Figure S6 in the Supporting Information). The fluorescence change was reproducible over several cycles of detection/stripping. The Job plot of the fluorescence changes indicated 1:1 binding for **1** with Zn^{2+} (Figure S7 in the Supporting Information). With the use of the fluorescence titration data, the association constant (K_a) for Zn^{2+} coordination to nanoparticle **1** was calculated to be $(2.31 \times 10^3) \text{ M}^{-1}$.^[13,14]

Spectral changes upon addition of the previously mentioned biologically and environmentally relevant metal ions were also screened by fluorophotometry. The emission profiles of apo or Zn^{2+} -bound **1** were unchanged in the presence of 10 μM Ca^{2+} , Hg^{2+} , Cd^{2+} , Li^+ , Ag^+ , Cu^{2+} , Fe^{2+} , Mg^{2+} , Pb^{2+} , K^+ , Na^+ , Mn^{2+} , Co^{2+} , Fe^{3+} , Al^{3+} , or Ni^{2+} (Figure 2b, and Figure S8 in the Supporting Information); this indicates that nanoparticle **1** shows great promise as a useful selective chemoprobe for detection of Zn^{2+} , in vivo.

Ideally, for biological applications, sensing should be practical over a range of pH values, and thus we investigated the effect of pH on the spectrophotometric behavior of nanoparticle **1** in both the absence and presence of Zn^{2+} (Figure S9 in the Supporting Information). Over the pH range from 3 to 11, nanoparticle **1** showed no fluorescence emission in the absence of Zn^{2+} , whereas upon the addition of Zn^{2+} , the fluorescence intensity of nanoparticle **1** was strongly dependent to pH values. The fluorescence intensity of nanoparticle **1** in the presence of Zn^{2+} was highest at pH 7.4. On the other hand, under acidic conditions, the fluorescence intensity of nanoparticle **1** slightly increased after addition of Zn^{2+} ; this can be attributed to protonation of the nitrogen atoms of ligand **2** immobilized on Fe_3O_4 nanoparticles.

To further demonstrate the practical application of the nanoparticle-based probe **1**, we established its ability to track Zn^{2+} levels in living cells using a model for respiratory zinc exposure. Live cell confocal microscope imaging experiments were carried out that utilized **1** to enhance membrane permeability (Figure 3a–c). HeLa cells (human cancer cells) were incubated with nanoparticle **1** (5.0 μM) for 30 min at 37 °C and then washed with phosphate buffered saline (PBS) to remove excess nanoparticle **1**, which would otherwise contribute to weak intracellular fluorescence (Figure 3B). On treating the cells with $\text{Zn}(\text{ClO}_4)_2$ (5.0 μM) for 30 min at 37 °C and then staining with nanoparticle **1** under the same loading conditions resulted in an increase in the observed intracellular fluorescence intensity of **1** (Figure 3C). This procedure allowed us to successfully perform selective Zn^{2+} imaging in living cells, despite the presence of many potential interfering substances, such as proteins and amino acids. Thus, nanoparticle **1** is potentially useful for studying the toxicity and/or bioactivity of Zn^{2+} in living cells. We further evaluated the internalization of **1** in HeLa cells by TEM (Figure S10 in the Supporting Information). Intact nanoparticles **1** within the cells are evident, as confirmed by measurement of their diameters. Conversely, few intact nanoparticles **1** are aggregated. This result provides

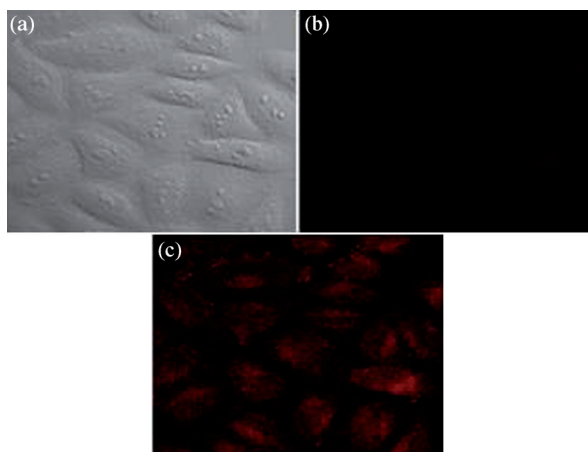


Figure 3. a) Bright-field confocal image of HeLa cells. b) Fluorescence image of HeLa cells incubated with **1** (5.0 μM) for 30 min at 37°C. c) Fluorescence image of **1**-loaded HeLa cells incubated with $\text{Zn}(\text{ClO}_4)_2$ (5.0 μM) after 30 min at 37°C.

visual evidence for cellular uptake of fluorescence receptor-immobilized Fe_3O_4 nanoparticles **1**.

Furthermore, we evaluated the reversibility of the above Zn^{2+} detection procedure in living cells (Figure S11 in the Supporting Information). The fluorescence emission of Zn^{2+} -bound **1** was observed to decrease to the initial level upon addition of EDTA (10 μM) to the HeLa cells. The fluorescence change was reproducible over several cycles of detection/stripping. This result strongly indicates that Zn^{2+} ions are dissociated from Zn^{2+} -bound **1** by EDTA. Clearly, chemoprobe **1** is not only very useful for detection and removal of toxic Zn^{2+} ions in living cells, but **1** is also readily regenerated by using the above procedure. This is a rare example of the reversible sensing of a target molecule or ions in living cells.

The cytotoxicity of **1** was evaluated against two different cell models: HeLa and Cos7 cells (monkey kidney fibroblasts; Figure 4). The two cell lines were chosen as representative models of the various cellular environments that **1** is likely to encounter, in vivo. In both cell lines, MTT (3-(4,5-dimethylthiazol-2-yl)-2,5-diphenyltetrazolium bromide) assays showed that nanoparticle **1** did not exhibit any toxicity at levels of up to 10 μM under same the conditions in which staurosporin (1.0 μM) induced 70–90% apoptotic cell death. These findings strongly suggest that the nanoparticles **1** are quite suitable as chemoprobes, in vivo, and they contrast markedly with the cationic polymers, amino- or polylysine-functionalized silica nanoparticles, which exhibit high toxicity in cell lines.

In summary, we have readily prepared BODIPY-functionalized Fe_3O_4 nanoparticles (**1**) by a straightforward procedure. These nanoparticles act as a new type of synthetic fluorogenic chemoprobe for imaging Zn^{2+} ions in living cells. Magnetic nanoparticle **1** exhibits a high affinity and selectivity for Zn^{2+} over other competing metal ions tested and they successfully detected Zn^{2+} in cultured cells. Furthermore, nanoparticle **1** did not exhibit any toxicity up to

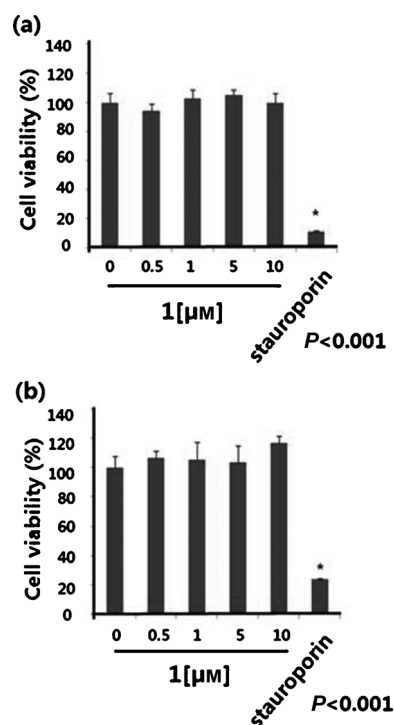


Figure 4. MTT cytotoxicity assay showing the effect of varying concentrations of **1** on growth inhibition of: a) HeLa, and b) Cos7 cell lines.

10 μM . These findings show considerable promise for the development of a new category of tailor-made biocompatible sensing systems built by immobilization of appropriate fluorogenic receptors on the surface of other novel nanomaterials for fluorescence microscopic imaging. They also show considerable promise for the detailed study of the biological action of heavy metal toxins in living systems.

Experimental Section

Preparation of Fe_3O_4 nanoparticles: Fe_3O_4 nanocrystals with 20 nm average core size were prepared by the previously reported procedure.^[15] Fe_3O_4 nanocrystals (80 mg) were dispersed in cyclohexane. Then, the resulting nanocrystals of Fe_3O_4 were collected by magnetic decantation. The collected nanocrystals of Fe_3O_4 were redispersed in EtOH and recovered by using a magnet. For purification, the dispersion of Fe_3O_4 into an EtOH suspension, followed by magnetic separation, was repeated three times.

Preparation of 2-immobilized Fe_3O_4 (1**):** Compound **2** (50 mg, 0.054 mmol) was dissolved in anhydrous toluene (5 mL) to which Fe_3O_4 nanoparticles (100 mg) were added. The mixture was stirred under reflux in N_2 for 24 h. The collected solid was washed several times with dichloromethane and acetone to rinse away any excess **2** and then dried under vacuum.

Cell incubation: HeLa cells were cultured in Dulbecco's modified Eagle's medium (DMEM, Gibco BRL, USA) supplemented with fetal bovine serum (FBS, 10%), penicillin (50 $\mu\text{g mL}^{-1}$), and streptomycin (50 $\mu\text{g mL}^{-1}$). The cells were grown on a microscopy culture dish (diameter, 35 mm) with poly-L-lysine coating. To determine the cell permeability of **1**, the cells were incubated with **1** (5.0 μM) for 30 min at 37°C, and washed with PBS to remove excess **1**. To observe fluorescence changes, $\text{Zn}(\text{ClO}_4)_2$ (5.0 μM) was added to the **1**-loaded cells and then further incu-

bated for 30 min at 37°C. Fluorescence changes was observed by confocal microscope. In addition, the reversibility of **1** loaded in HeLa cell was observed by treatment with EDTA solution (10 μM).

TEM of **1 loaded in HeLa cells:** Compound **1**-loaded HeLa cells were cultured on poly-L-lysine-coated glass-bottom dishes (diameter, 35 mm) and loaded with nanoparticle **1** for 30 min. The cells were fixed with glutaraldehyde (2.5%) in phosphate buffer (0.1 M), postfixed with OsO₄ (1%) for 1 h. Dehydrated specimens were embedded in Epon 812. The polymerized blocks were cut at 70 nm, contrasted with uranyl acetate and lead citrate and analyzed with a Tecnai G2 Spirit Twin TEM (FEI, USA).

MTT cell viability assay: Assays were performed according to the manufacturer's protocol (EZ-Cytox, Dail Lab Service). Briefly, HeLa and Cos7 cells were treated with the nanoparticles or staurosporin for 24 h, incubated with MTT reagent for 1 h at 37°C and the MTT assay was carried out.

Fluorescence imaging experiments: Confocal fluorescence imaging was performed with a Zeiss LSM510 Meta laser scanning microscope and a 40× oil-immersion objective lens, by using image Pro Plus 5.1 software. Excitation of **1**-loaded cells at 635 nm was carried with HeNe laser, and emission was acquired at over 650 nm range. For all images, the microscopy incubation chamber (Chamlide TC, LCI, Korea) was used at 37°C in 5% CO₂, humidified air.

Acknowledgements

This work was supported by a grant from Environmental-Fusion Project (191-091-004), and World Class Project (WCU) supported by Ministry of Education Science and Technology, Korea (R32-2008-000-20003-0 and NRF-2011-0006393). In addition, this work was partially supported by a grant from the Next-Generation BioGreen 21 Program (SSAC, PJ008109), of the Rural Development Administration, S. Korea.

Keywords: biosensors • chromophores • fluorophores • nanoparticles • zinc

- [1] a) A. W. Cramik, *Fluorescent Chemosensors for Ion and Molecular Recognition*, American Chemical Society, Washington, DC, **1993**; b) A. P. de Silva, H. Q. N. Gunaratne, T. Gunnlaugsson, A. J. M. Huxley, C. P. McCoy, J. T. Rademacher, T. E. Rice, *Chem. Rev.* **1997**, *97*, 1515; c) R. Martínez-Mañez, F. Sancanon, *Chem. Rev.* **2003**, *103*, 4419; d) T. Gunnlaugsson, M. Glynn, G. M. Tocci, P. E. Krüge, F. M. Pfeffer, *Coord. Chem. Rev.* **2006**, *250*, 3094.
- [2] a) S. C. Burdette, G. K. Walkup, B. Spingler, R. Y. Tsien, S. J. Lippard, *J. Am. Chem. Soc.* **2001**, *123*, 7831; b) P. Jiang, L. Chen, J. Lin, Q. Liu, J. Ding, X. Gao, Z. Guo, *Chem. Commun.* **2002**, 1424; c) S. Ko, Y. Yang, J. Tae, I. Shin, *J. Am. Chem. Soc.* **2006**, *128*, 14150; d) M. Taki, M. Desaki, A. Ojida, S. Lyoshi, T. Hirayama, I. Hamachi, Y. Yamamoto, *J. Am. Chem. Soc.* **2008**, *130*, 12564; e) X. Zhang, Y. Xiao, X. Qian, *Angew. Chem.* **2008**, *120*, 8145; *Angew. Chem. Int. Ed.* **2008**, *47*, 8025.
- [3] a) B. L. Vallee, K. H. Falchuk, *Physiol. Rev.* **1993**, *73*, 79; b) D. S. Auld, *Biomaterials* **2011**, *14*, 271.
- [4] a) S. J. Lippard, J. M. Berg, *Principle of Bioinorganic Chemistry*, University Science Books, Mill Valley, **1994**, pp. 10, 14, 78; b) E. M. Nolan, S. J. Lippard, *Acc. Chem. Res.* **2009**, *42*, 193.
- [5] a) K. Hanaoka, K. Kikuchi, H. Kojima, Y. Urano, T. Nagano, *J. Am. Chem. Soc.* **2004**, *126*, 12470; b) M. Royzen, A. Durandin, V. G. Young, N. E. Geachintov, J. W. Canary, *J. Am. Chem. Soc.* **2006**, *128*, 3854; c) R. Parkesh, T. C. Lee, T. Gunnlaugsson, *Org. Biomol. Chem.* **2007**, *5*, 310; d) Y. Liu, N. Zhang, Y. Chen, L. Wang, *Org. Lett.* **2007**, *9*, 315; e) H. Wang, Q. Gan, X. Wang, L. Xue, S. Liu, H. Jiang, *Org. Lett.* **2007**, *9*, 4995; f) Y. Zhang, X. Guo, W. Si, L. Jia, X. Qian, *Org. Lett.* **2008**, *10*, 473; g) L. Xue, C. Liu, H. Liang, *Org. Lett.* **2009**, *11*, 1655; h) J. Wang, C. Ha, *Tetrahedron* **2009**, *65*, 6959.
- [6] Z. Xu, K. H. Beak, H. N. Kim, J. Cui, X. Qian, D. R. Spring, I. Shin, J. Yoon, *J. Am. Chem. Soc.* **2010**, *132*, 601.
- [7] a) Y. H. Zhu, H. Da, X. L. Yang, Y. Hu, *Colloid. Surface. A* **2003**, *231*, 123; b) D. K. Yi, S. T. Selvan, S. S. Lee, G. C. Papaefthymiou, *J. Am. Chem. Soc.* **2005**, *127*, 4990.
- [8] a) J. H. Jung, J. H. Lee, S. Shinkai, *Chem. Soc. Rev.* **2011**, *40*, 4464; b) H. Son, H. Y. Lee, J. M. Lim, D. Kang, W. S. Han, S. S. Lee, J. H. Jung, *Chem. Eur. J.* **2010**, *16*, 11549; c) M. Park, S. Seo, I. S. Lee, J. H. Jung, *Chem. Commun.* **2010**, 46, 4478; d) H. Y. Lee, D. R. Bae, J. C. Park, H. Song, W. S. Han, J. H. Jung, *Angew. Chem.* **2009**, *121*, 1265; *Angew. Chem. Int. Ed.* **2009**, *48*, 1239.
- [9] X. Peng, J. Du, J. Fan, J. Wang, Y. Wu, J. Zhao, S. Sun, T. Xu, *J. Am. Chem. Soc.* **2007**, *129*, 1500.
- [10] a) A. Loudet, K. D. Burgess, *Chem. Rev.* **2007**, *107*, 4891; b) A. Coskun, E. U. Akkaya, *J. Am. Chem. Soc.* **2005**, *127*, 10464; c) K. Rurack, M. Kollmannsberger, J. Daub, *Angew. Chem.* **2001**, *113*, 396; *Angew. Chem. Int. Ed.* **2001**, *40*, 385.
- [11] Z. Ekmekci, M. D. Yilmaz, E. U. Akkaya, *Org. Lett.* **2008**, *10*, 461.
- [12] J. E. Huheey, E. A. Keiter, R. L. Keiter, *Inorganic Chemistry*, Harper Collins, **1993**, p. 344.
- [13] Association constants were obtained by using the computer program ENZFITTER, available from Elsevier-BIOSOFT: <http://www.biosoft.com/w/enzfitter.htm>
- [14] K. A. Connors, *Binding Constants, The Measurement of Molecular Complex Stability*, Wiley, New York, **1987**.
- [15] J. Park, K. An, Y. Hwang, J.-G. Park, H.-J. Noh, J.-Y. Kim, J.-H. Park, N.-M. Hwang, T. Hyeon, *Nat. Mater.* **2004**, *3*, 891.

Received: January 27, 2012
Published online: April 19, 2012